



HAL
open science

Evaluation of a photorefractive two beam coupling novelty filter

Philippe Delaye, Gérald Roosen

► **To cite this version:**

Philippe Delaye, Gérald Roosen. Evaluation of a photorefractive two beam coupling novelty filter. Optics Communications, 1999, 165, pp.133-151. 10.1016/S0030-4018(99)00200-X . hal-00673971v2

HAL Id: hal-00673971

<https://hal-iogs.archives-ouvertes.fr/hal-00673971v2>

Submitted on 30 Mar 2012

HAL is a multi-disciplinary open access archive for the deposit and dissemination of scientific research documents, whether they are published or not. The documents may come from teaching and research institutions in France or abroad, or from public or private research centers.

L'archive ouverte pluridisciplinaire **HAL**, est destinée au dépôt et à la diffusion de documents scientifiques de niveau recherche, publiés ou non, émanant des établissements d'enseignement et de recherche français ou étrangers, des laboratoires publics ou privés.

EVALUATION OF A PHOTOREFRACTIVE TWO BEAM COUPLING NOVELTY FILTER

Philippe Delaye, Gérald Roosen

Laboratoire Charles Fabry, Unité Mixte de Recherche 8501 du Centre National de la
Recherche Scientifique et de l'Institut d'Optique Théorique et Appliquée, Bat. 503, Centre
Scientifique d'Orsay, B.P. 147, 91403 Orsay Cedex, France.

Tel : 33-1-69-35-87-50, Fax : 33-1-69-35-87-00, Email : Philippe.delaye@iota.u-psud.fr

Abstract :

Theoretical and experimental study of a novelty filter is presented. We show that best performances are obtained when the images are presented to the set-up with a spatial light modulator operating as a linear phase modulator. We obtained a good accordance between the experimental curves and the calculated ones, what validates the model we develop for this novelty filter.

A novelty filter is an image pre-processing element that is sensitive only to the new features in a scene. It is thus perfectly adapted to the detection of an object appearing and moving in a complex scene. Different architectures were proposed to implement a novelty filter with a photorefractive crystal [1-4]. They use phase conjugation [2], ring geometries [2], two beam coupling energy transfer [1,2] or even beam fanning [1]. Among these different set-ups the last two are very simple to implement. Nevertheless, the beam fanning novelty filter is not adapted to our problem as it is not a true differentiating set-up [1] (for example it would not be sensitive to a uniform phase change of the image). That's why we choose the two beam coupling novelty filter. A signal beam carrying the image (i.e. the complex scene) interferes with a pump beam in a high gain photorefractive crystal. Energy transfer occurs through two beam coupling that causes a strong attenuation of the stationary signal beam. As soon as an object appears or moves in the scene the attenuation condition is no more fulfilled and light passes immediately at the location of the object, and only there, until a new grating is written what restores attenuation. Such a system allows thus to detect very small moving objects, with very small contrasts compared to the textured background.

The aim of this paper is to describe both theoretically and experimentally the operation of a two beam coupling novelty filter, with the objective to detect the smallest possible grey level variation ($\Delta n=1$) on an arbitrary background. In a first part we will model this device, showing that the best operating conditions are obtained with an image coded on the beam as a phase modulation. In the second part we will describe the experimental set-up and its characterization. Last part will compare experimental results with theory showing an excellent agreement that enables to predict the performances of future systems using optimized components.

I. THEORETICAL BACKGROUND

The principle of the two beam coupling novelty filter is based on a classical two beam coupling set-up (Fig. 1). A signal beam E_d carrying the information of an image imprinted on it is sent on a photorefractive crystal, with a coherent pump beam E_i . Both beams interfere and write through the photorefractive effect an hologram of the signal beam wavefront. The crystal is used in such a way that the signal beam transfers its energy toward the pump beam leading to a strong depletion of it. This attenuation is due to a quasi perfect destructive interference between the transmitted signal beam and the diffracted pump beam [1,2]. At a given time, the imprinted image is locally changed much rapidly than the response time of the photorefractive crystal. The transmitted image accordingly changes its wavefront whereas the hologram and thus the diffracted pump beam does not have the time to adapt to this change. The condition of destructive interference is no more fulfilled in all the parts of the image that have changed. There is no more attenuation in these locations that reappears suddenly as

bright spots in the attenuated image field. After some time, the crystal adapts itself to the new wavefront by writing a new hologram leading again to the attenuation of the whole signal beam.

If we look at this description more closely, we see that we have to consider the transmission of a time modulated signal beam in a two beam coupling set-up, with a pump beam that is stationary and not depleted (it just acquires a small quantity of energy from the much weaker signal beam through beam coupling process). We can thus apply the theoretical model we previously developed [5] and we already successfully used for the description of the photorefractive two beam coupling ultrasonic detector [6,7]. This model is derived from the one used in Ref. [1] (it takes into account the absorption of the photorefractive crystal that causes changes of the photorefractive time constant during the propagation through the crystal). It is also equivalent to the Laplace transform formalism used in Ref. [2], except in the final evaluation of the inverse Laplace transform, for which we prefer the convolution calculation, we estimated more adapted to our problem and easier to use.

The time modulated signal beam $E_d(0,t)$ is sent on a photorefractive crystal having a photorefractive gain in amplitude γ , an absorption coefficient α and a thickness x . The photorefractive time constant at the entrance of the crystal is τ_0 . In the condition in which the crystal is used, i.e. a photorefractive crystal in the diffusion regime, gain γ is real and negative (to account for an energy transfer from the signal towards the pump) and the photorefractive time constant τ_0 is real. Finally we suppose that a photorefractive grating is written in its steady state regime when the change of the image occurs at time $t=0$.

Taking into account all these considerations, the transmission of the time modulated signal beam through the crystal is governed by the following equation [5]:

$$E_d(x,t) = e^{-\frac{\alpha x}{2}} e^{\gamma x} \left[E_d(0,0) + \int_0^t \left(\tau_0 \frac{\partial E_d}{\partial t}(0,T) + E_d(0,T) - E_d(0,0) \right) H(x,t-T) dT \right] \quad (1)$$

with $H(x,t) = \frac{e^{\gamma x}}{\tau_0} e^{-\frac{t}{\tau_0}} {}_1F_1\left(\frac{\gamma}{\alpha}, 1, \left(\frac{e^{\alpha x} - 1}{e^{\alpha x}}\right) \frac{t}{\tau_0}\right)$ and ${}_1F_1(a, b, z)$ the confluent hypergeometric function [8].

This expression is complex but perfectly usable as the hypergeometric function is known and tabulated. Nevertheless, the fact that the expression uses the derivative of $E_d(0,t)$ might bring a difficulty in the interpretation. This is why, using an integration by parts and defining function $G(x,t) = e^{\gamma x} \left[H(x,t) + \tau_0 \frac{\partial H}{\partial t}(x,t) \right]$, we rewrite equation (1) [9,7] taking into account the properties of hypergeometric function [8] :

$$E_d(x,t) = e^{-\frac{\alpha x}{2}} \left[(E_d(0,t) - E_d(0,0)) + E_d(0,0) e^{\gamma x} + \int_0^t (E_d(0,T) - E_d(0,0)) G(x,t-T) dT \right] \quad (2)$$

with $G(x,t) = \left(\frac{e^{\alpha x} - 1}{\tau_0 e^{\alpha x}} \right) \frac{\gamma}{\alpha} e^{-\frac{t}{\tau_0}} {}_1F_1\left(\frac{\gamma + \alpha}{\alpha}, 2, \left(\frac{e^{\alpha x} - 1}{e^{\alpha x}}\right) \frac{t}{\tau_0}\right)$.

Thus using equation (2) and knowing the expression of $E_d(0,t)$ at the entrance of the crystal, we now deduce its expression at the output.

Signal $E_d(0,t)$ presented at the entrance can be split into two parts : a constant part $E_{d0}(0,t)=E_d(0,0)$ and a varying part $\Delta E_d(0,t)$ that is different from zero only for $t>0$. Expression (2) being linear, the response of the system is equal to :

$$E_d(x,t) = E_{d0}(x,t) + \Delta E_d(x,t) \quad (3)$$

The response of each part being given by equation (2).

We thus have :

$$E_{d0}(x,t) = E_d(0,0)e^{-\frac{\alpha x}{2}}e^{\gamma x} = E_0 e^{-\frac{\alpha x}{2}}e^{\gamma x} \quad (4)$$

and :

$$\Delta E_d(x,t) = e^{-\frac{\alpha x}{2}} \left[\Delta E_d(0,t) + \int_0^t \Delta E_d(0,T)G(x,t-T)dT \right] \quad (5)$$

Which gives :

$$E_d(x,t) = e^{-\frac{\alpha x}{2}} \left[E_0 e^{\gamma x} + \Delta E_d(0,t) + \int_0^t \Delta E_d(0,T)G(x,t-T)dT \right] \quad (6)$$

The response will thus depend on the temporal variation of the input signal. To modelize the working of the novelty filter, we consider a perfect impulse variation of the amplitude of the entrance signal beam having a duration Δt and amplitude ΔE , given by :

$$\begin{cases} \Delta E_d(0,t) = 0 & t \leq 0 \\ \Delta E_d(0,t) = \Delta E & 0 < t \leq \Delta t \\ \Delta E_d(0,t) = 0 & t > \Delta t \end{cases} \quad (7)$$

that we can rewrite, using the Heavyside function $U(t)$ ($U(t)=1$ for $t > 0$, $U(t)=0$ elsewhere) :

$$\Delta E_d(0,t) = \Delta E U(t) - \Delta E U(t - \Delta t) = \Delta E (U(t) - U(t - \Delta t)) \quad (8)$$

We introduce now $\Delta E_d(0,t)$ in equation (5), what gives :

$$\Delta E_d(x,t) = \Delta E e^{-\frac{\alpha x}{2}} \left[U(t) - U(t - \Delta t) + \int_0^t U(t-T)G(x,T)dT + \int_0^{t-\Delta t} U(t-T-\Delta t)G(x,T)dT \right] \quad (9)$$

Taking into account the properties of the Heavyside function, both integrals can be rewritten :

$$\Delta E_d(x,t) = \Delta E e^{-\frac{\alpha x}{2}} \left[U(t) - U(t - \Delta t) + \int_0^t G(x,T)dT + \int_0^{t-\Delta t} G(x,T)dT \right] \quad (10)$$

What gives in final :

$$\begin{cases} \Delta E_d(x,t) = 0 & t \leq 0 \\ \Delta E_d(x,t) = \Delta E e^{-\frac{\alpha x}{2}} \left[1 + \int_0^t G(x,T) dT \right] & 0 < t \leq \Delta t \\ \Delta E_d(x,t) = \Delta E e^{-\frac{\alpha x}{2}} \int_{t-\Delta t}^t G(x,T) dT & t > \Delta t \end{cases} \quad (11)$$

We define a function $R(t,\Delta t) = \int_{t-\Delta t}^t G(x,T) dT$ what allows to write $R(t,t) = \int_0^t G(x,T) dT$. We can now come back to the total amplitude of the signal $E_d(x,t)$:

$$\begin{cases} E_d(x,t) = E_0 e^{-\frac{\alpha x}{2}} e^{\gamma x} & t \leq 0 \\ E_d(x,t) = E_0 e^{-\frac{\alpha x}{2}} e^{\gamma x} + \Delta E e^{-\frac{\alpha x}{2}} [1 + R(t,t)] & 0 < t \leq \Delta t \\ E_d(x,t) = E_0 e^{-\frac{\alpha x}{2}} e^{\gamma x} + \Delta E e^{-\frac{\alpha x}{2}} R(t, \Delta t) & t > \Delta t \end{cases} \quad (12)$$

The response of the novelty filter will thus depend on the parameters of the crystal, and on the characteristics of the amplitude variation.

The normal application of the novelty filter is the detection of very rapid fluctuations of the signal beam, compared to the response time of the photorefractive crystal. In order to consider the performances of the novelty filter, we will thus be in these normal conditions of operation of the novelty filter. We consequently suppose that $\Delta t \ll \tau_0$ (and thus that we make a measurement on a time period much smaller than the response time of the crystal $t \ll \tau_0$). This means that the function $G(x,t)$ that appears in the definition of the functions $R(t,\Delta t)$ does not vary and stays equal to its value at time $t=0$:

$$G(x,t) \approx G(x,0) = \left(\frac{e^{\alpha x} - 1}{\tau_0 e^{\alpha x}} \right) \frac{\gamma}{\alpha} \quad (13)$$

$$\text{as } {}_1F_1\left(\frac{\gamma + \alpha}{\alpha}, 2, 0\right) = 1$$

It means that we have :

$$R(t,t) = \int_0^t G(x,T) dT \approx \int_0^t G(x,0) dT = \left(\frac{e^{\alpha x} - 1}{e^{\alpha x}} \right) \frac{\gamma}{\alpha} \frac{t}{\tau_0} \approx 0 \quad (14)$$

since $t \ll \tau_0$.

In the same manner, we have $R(t,\Delta t) \approx 0$

This means that expression (12) becomes :

$$\begin{cases} E_d(x,t) = E_0 e^{-\frac{\alpha x}{2}} e^{\gamma x} & t \leq 0 \\ E_d(x,t) = E_0 e^{-\frac{\alpha x}{2}} e^{\gamma x} + \Delta E e^{-\frac{\alpha x}{2}} & 0 < t \leq \Delta t \\ E_d(x,t) = E_0 e^{-\frac{\alpha x}{2}} e^{\gamma x} & t > \Delta t \end{cases} \quad (15)$$

We see on this expression the response of the novelty filter to a variation ΔE of the amplitude of the signal beam. In the normal operation of the filter we choose the photorefractive gain such that we have $\Delta E \gg E_0 e^{\gamma x}$. In this condition the output exactly reproduces the signal variation (except for the reduction due to the absorption of the crystal), and we have :

$$\begin{cases} E_d(x, t) \approx 0 & t \leq 0 \\ E_d(x, t) = \Delta E e^{-\frac{\alpha x}{2}} & 0 < t \leq \Delta t \\ E_d(x, t) \approx 0 & t > \Delta t \end{cases} \quad (16)$$

This result is obtained in perfect conditions of a photorefractive crystal having a very strong photorefractive gain γ and a very slow response time compared to the duration of the novelty. The reality is somewhat different. To analyse the effect of the material response time, we have to go back to equation (12) to know the temporal response of the novelty filter and the rate at which the filter will readapt to the signal change, when this change is not short compared to the response time of the photorefractive crystal. For the effect of a limited value of the photorefractive gain on the response and its choice in order to have an attenuation sufficient to obtain the desired response, the analysis is less direct. In fact looking further to what happens in the novelty filter, we will have to take into account the exact nature of the amplitude change ΔE . Indeed the image can be imprinted on the signal beam in two different ways : first it can be imprinted as an intensity modulation where the image levels correspond to different intensity levels of the beam, second it can be coded as a phase modulation where the image levels correspond to local changes of the phase of the beam. Performances of the novelty filter will be analyzed in both cases.

I.1. Intensity modulation case

The image is coded as an intensity variation of the beam. Thus a novelty will be seen as a local variation of the intensity of the beam from an intensity level I_0 towards a new level $I_0 + \Delta I$. Then according to the previous notations we have :

$$\Delta E = \sqrt{I_0 + \Delta I} - \sqrt{I_0} \quad (17)$$

In order to have an optimum response of the novelty filter, we need to have (equation (15)) :

$$E_0 e^{\gamma x} \ll \Delta E \quad (18)$$

and thus :

$$e^{\gamma x} \ll \sqrt{\frac{I_0 + \Delta I}{I_0}} - 1 = \sqrt{1 + \frac{\Delta I}{I_0}} - 1 \quad (19)$$

we see that the requirement on the photorefractive gain γ depends on the initial intensity I_0 .

We thus have to take into account the coding of the image. We here take the example of an image linearly coded with N grey levels. Thus $I_0 = n I_G$, with $0 \leq n < N$, and I_G the intensity variation corresponding to a variation of one grey level. Taking into account inequality (19), the most difficult signal to measure will thus correspond to a measurement of a variation of one grey level (smallest ΔI , i.e. $\Delta I = I_G$), on a high level (i.e. $I_0 \approx N I_G$). Inequality (19) then becomes :

$$e^{\gamma x} \ll \sqrt{1 + \frac{1}{N}} - 1 \quad (20)$$

Practically, there is a large number of grey level such as $N \gg 1$ and then :

$$e^{\gamma x} \ll \frac{1}{2N} \quad (21)$$

To give an idea of the constraint on the photorefractive gain we take the example of an image coded on 256 level (8 bit images), then a gain γ such that $e^{\gamma x} \approx \frac{1}{5000}$ should be sufficient to verify relation (21). This corresponds to an attenuation (given by $e^{-2\gamma x}$) of the initial signal beam of the order of 2.5×10^7 . In order to have such a high exponential gain with a 0.5cm thick crystal, an intensity photorefractive gain $\Gamma = 2\gamma$ of the order of 35cm^{-1} is needed. This is high but accessible with a baryum titanate crystal [10]. Nevertheless such an attenuation would be very difficult to obtain experimentally because of the imperfections of the set-up (residual phase modulation due to vibrations, scattering on the crystal defects, ...).

Considering this optimum conditions fulfilled, the response of the novelty filter is given by equation (16). Then the intensity change at the output in response to the entrance intensity change is equal to :

$$|\Delta E|^2 = \left| \sqrt{I_0 + \Delta I} - \sqrt{I_0} \right|^2 = 2I_0 + \Delta I - 2\sqrt{I_0(I_0 + \Delta I)} \quad (22)$$

In the normal utilization case, we need to measure a small intensity variation on a moderate background, we thus have $\Delta I \ll I_0$. Then the response becomes :

$$|\Delta E|^2 = \frac{\Delta I^2}{4I_0} \quad (23)$$

This response is not at all linear and it depends both on the incident intensity variation ΔI and on the initial level I_0 on which the variation is applied. Detection of variation of 1 grey level will be easier on a black level than on a white one as the response depends on the initial level I_0 .

To characterize the response of the novelty filter we define the novelty factor (sometimes called with the ambiguous term contrast [2]) as the ratio of the intensity of the transmitted signal beam during the novelty to the intensity of the transmitted signal just before the change :

$$C = \frac{I_d(x, 0 < t \leq \Delta t)}{I_d(x, t \leq 0)} = \frac{|\Delta E|^2}{I_0 e^{2\gamma x}} = e^{-2\gamma x} \left| \frac{\Delta E}{\sqrt{I_0}} \right|^2 = e^{-2\gamma x} \left| \frac{\sqrt{I_0 + \Delta I}}{\sqrt{I_0}} - 1 \right|^2 \quad (24)$$

As $\Delta I \ll I_0$, this novelty factor becomes $C = e^{-2\gamma x} \left(\frac{\Delta I}{2I_0} \right)^2$.

Without the novelty filter the same ratio can be defined. Its value is then :

$$C' = \frac{I_0 + \Delta I}{I_0} \quad (25)$$

which gives, as $\Delta I \ll I_0$, $C' = 1$.

We see that the novelty filter brings a gain in the novelty factor of the order of the attenuation rate $e^{-2\gamma x}$ in the measurement of the intensity variation of the signal beam. Such a gain will be very strong if we can obtain the expected attenuation of 2.5×10^7 required for an optimum operation of the novelty filter with an intensity modulated beam.

I.2. Phase modulation case

We have just seen that with an intensity modulated signal beam, the response of the novelty filter depends on the initial level from which the variation is made. This important drawback does not exist in the case of a phase modulated beam. Indeed the grating written by the interference of the pump beam and the signal beam, carries the information on the spatial variation of the phase φ_0 of the signal beam. Diffraction on the grating will give a wave that will carry this phase information, to which will be added a constant phase shift of π (independantly of the initial phase φ_0) that will be responsible of the attenuation of the signal beam. The local value of the phase φ_0 can thus vary without any influence on the transmitted beam. The novelty filter only uses the fact that the diffracted beam is π phase shifted compared to the transmitted beam and that whatever the initial phase of the transmitted beam. The system reacts to a phase variation $\Delta\varphi$ from an initial phase φ_0 . As the transmitted beam as no reference concerning the exact value of the phase φ_0 , the system can not distinguish a phase variation from a level φ_0 , from that from a level φ'_0 . We will thus measure in the same manner a phase variation on a “black” level or on a “white” level, what is very interesting for an actual application of the novelty filter.

Going back to the previous expressions, the initial amplitude is $E_0 = \sqrt{I_0} e^{i\varphi_0}$, whereas the amplitude after the change is $E_1 = \sqrt{I_0} e^{i\varphi_1} = \sqrt{I_0} e^{i(\varphi_0 + \Delta\varphi)}$. The amplitude variation is then :

$$\Delta E = \sqrt{I_0} e^{i\varphi_0} (e^{i\Delta\varphi} - 1) \quad (26)$$

Then between 0 and Δt , we have (equation (15)) :

$$E_d(x, t) = \sqrt{I_0} e^{i\varphi_0} e^{-\frac{\alpha x}{2}} (e^{\gamma x} + e^{i\Delta\varphi} - 1) \quad (27)$$

which gives an intensity :

$$I_d(x, t) = I_0 e^{-\alpha x} \left(e^{2\gamma x} - 4 e^{\gamma x} \sin^2 \frac{\Delta\varphi}{2} + 4 \sin^2 \frac{\Delta\varphi}{2} \right) \quad (28)$$

The photorefractive gain γ has to be chosen such that the first two terms of expression (28) are negligible compared to the last one. This gives two conditions :

$$\begin{cases} e^{2\gamma x} \ll 4 \sin^2 \frac{\Delta\varphi}{2} \\ 4 e^{\gamma x} \sin^2 \frac{\Delta\varphi}{2} \ll 4 \sin^2 \frac{\Delta\varphi}{2} \end{cases} \Rightarrow \begin{cases} e^{2\gamma x} \ll 4 \sin^2 \frac{\Delta\varphi}{2} \\ e^{\gamma x} \ll 1 \end{cases} \quad (29)$$

The second condition is generally automatically verified when the first one is. In the case of the detection of small phase shift variations ($\Delta\varphi \ll \pi$), this first condition becomes :

$$e^{2\gamma x} \ll \Delta\varphi^2 \quad (30)$$

where $\Delta\varphi$ is the smallest phase shift variation we want to measure. For a modulator giving a linear phase modulation with a maximum value of $k\pi$ radians with N grey levels, we have $\Delta\varphi = k\pi/N$, and the condition becomes :

$$e^{2\gamma x} \ll \left(\frac{k\pi}{N}\right)^2 \quad (31)$$

for a maximum induced phase shift of π ($k=1$) and $N=256$ grey levels, this gives :

$$e^{2\gamma x} \ll \frac{1}{6600} \quad (32)$$

Thus an attenuation of the order of 6×10^4 should be sufficient to have an optimum response of the novelty filter. This is almost three order of magnitude smaller than in the case of the intensity modulation. This difference is due to the fact that here the condition is directly on the attenuation $e^{2\gamma x}$ rather than on its square root as in the case of the intensity modulation. This attenuation corresponds to a gain of 22 cm^{-1} for a 0.5 cm thick crystal, which is readily available experimentally with baryum titanate crystals [10].

Considering now that we have this optimum value of the gain, the intensity variation giving the response of the system is given by the last term of equation (28) and equals :

$$|\Delta E|^2 = 4I_0 \sin^2 \frac{\Delta\varphi}{2} \quad (33)$$

This response depends linearly with I_0 as the signal received by the detector is proportional to the constant power sent to the crystal. The independence compared to the initial level is here given by the independence of equation (33) with respect to the initial phase φ_0 . In the case where $\Delta\varphi/2 \ll \pi/2$, we have :

$$|\Delta E|^2 = I_0 \Delta\varphi^2 \quad (34)$$

From this we obtain the novelty factor C which value is :

$$C = \frac{I_d(x, 0 < t \leq \Delta t)}{I_d(x, t \leq 0)} = \frac{|\Delta E|^2}{I_0 e^{2\gamma x}} = 4e^{-2\gamma x} \sin^2 \frac{\Delta\varphi}{2} \approx e^{-2\gamma x} \Delta\varphi^2 \quad (35)$$

If we compare this response to the one obtained in the case of intensity modulation, we still have a quadratic response of the novelty filter but now the response is completely independent of the initial state of the image. Moreover this optimum operation of the novelty

filter is obtained with a less tough, and easier to obtain, condition on the required attenuation. Consequently a novelty filter which aim is to detect small changes in a complexe image, whatever its exact structure, will be much better and easier to implement if the image is imprinted on the beam as a phase modulation.

I.3. Problems linked to the use of a phase modulated beam

As we have seen, taking into account the response of the novelty filter, it is extremely advantageous to work with images coded as a phase modulation. This response will be all the more efficient as the phase variation induced by a variation of one grey level will be important. We thus see that it can be advantageous to boost the response of the Spatial Light Modulator (SLM) to have it giving a maximum phase equal to $k\pi$ with k greater than one. Nevertheless such a modulation range would bring some drawbacks, essentially due to the sinusoidal response of the novelty filter. In such a case (taking $k>1$) the system is very sensitive to small grey level variations but can be completely insensitive to very high variations of grey level (for example if we have a variation such that $\Delta\varphi=2\pi$ we then have $\Delta E=0$). This point has to be taken into account in the design of the novelty filter, i.e. the choice of the SLM will depend on the final use of the novelty filter.

This problem of the cancellation of the response at high novelty phase shifts (around $\Delta\varphi\approx 2\pi$) has nevertheless to be moderated. Indeed when establishing the expressions for the response of the novelty filter, we supposed that the phase change was instantaneous (illustrated by the use of a heavyside function). In reality this change will not be as sudden. Indeed the SLM needs a certain time to commute from one value φ_0 to another φ_1 . During this time all the phase values will be seen, giving a non zero response of the novelty filter. If we come back to the case of a phase variation between 0 and 2π , we will thus have a transient response that gives a signal even if the steady state response is zero. To simulate this effect we can not use the previous expressions (12) as they correspond to a sudden phase shift change. We thus have to come back to the initial expression (2) using $E_d(0, t) = E_0 e^{i\varphi(t)}$ with $\varphi(t)$ reproducing the exact response of the SLM. In our case we use an exponential response of the SLM with a time constant τ_R , which gives for the phase modulation :

$$\begin{cases} \varphi(0, t) = \varphi_0 & t \leq 0 \\ \varphi(0, t) = (\varphi_1 - \varphi_0) \left(1 - e^{-\frac{t}{\tau_R}} \right) + \varphi_0 & 0 < t \leq \Delta t \\ \varphi(0, t) = (\varphi_1 - \varphi_0) \left(e^{-\frac{(t-\Delta t)}{\tau_R}} \right) + \varphi_0 & \Delta t < t \end{cases} \quad (36)$$

The result of such a calculation is showed in Fig. 2 (only the first transition is shown, an equivalent response would be given for the second one). We see that if the phase transition

is important we observe a transient response which width is characteristics of the response time of the SLM, but which height is rather constant. We thus have the possibility to detect a signal even if the phase modulation is equal to 2π . The exact interpretation of the response can be complex but because of the non instantaneous response time of the SLM we have the possibility to enhance the response of the novelty filter to small variation of the grey level, without missing any higher variation.

The finite response time of the SLM has another effect that is seen in Fig. 2.A, giving the amplitude of the response at small phase variations. The height of the peak will be all the more high as the time constant of the SLM will be short compared to the response time of the novelty filter. This comes from a partial adaptation of the hologram during the phase change when the phase is changed “slowly”, giving a reduced response of the novelty filter.

With this model we can simulate the response of the novelty filter. For this we just have to introduce the exact expression of the novelty at the entrance of the crystal, in equation (2) and calculate the response of the novelty filter. Peculiar characteristics of the SLM (noise, mixed amplitude-phase response or response time of the SLM) can be also introduced and taken into account to describe the response of the system.

I.4. Discussion

We have shown in this theoretical part that it is very advantageous for the operation of a photorefractive novelty filter to imprint the images in the set-up as a phase modulation of the signal beam. Indeed, in such a case, we have a response to the grey level variation that is completely independent of the initial grey level. It is thus as easy to detect a one grey level change on a “black” image as on a “white” level. Moreover, the experimental conditions necessary to obtain an “ideal” condition of use of the novelty filter are less stringent than for an intensity modulated image. A less strong attenuation is required and then a smaller photorefractive gain is necessary for the crystal.

Before presenting the comparison of the experimental results with the calculated curves obtained from the theoretical model, we will describe the experimental set-up of the two beam coupling photorefractive novelty filter we implemented.

II. EXPERIMENTAL IMPLEMENTATION OF THE PHOTOREFRACTIVE NOVELTY FILTER

II.1. Experimental set-up

The basis of the experimental set-up is a two beam coupling experiment (Fig. 3). The laser source is a single mode Argon laser emitting at $\lambda=514\text{nm}$. The beam is split in two beams by a polarizing beam splitter, the respective power between the two beams being adjusted by a $\lambda/2$ plate. The signal beam is filtered and expanded to illuminate uniformly the

spatial light modulator (SLM). Two $\lambda/2$ plate before and after the SLM adjust the polarization and a dichroic polarizer just before the crystal is used to accurately select an extraordinary polarization. An afocal system made with achromats makes the image of the SLM in the vicinity of the photorefractive crystal, image that is again taken by another afocal to form a final image on a CCD camera. A pinhole in the Fourier plane of the second afocal allows to transmit only the zeroth order of the diffraction pattern due to the pixelated structure of the SLM. This pinhole also eliminates some of the scattered light issued from the pump beam that can reach the CCD camera. When temporal response is to be measured, the CCD camera is replaced by a Si detector. The pump beam is also extraordinary polarized and expanded to uniformly cover the image of the SLM, which was about $3 \times 3 \text{ mm}^2$. Most of the energy of the laser was sent in the pump beam which power at the level of the photorefractive crystal was typically around 3 W.cm^{-2} . The power of the signal beam was small enough to have a pump to signal power ratio at the entrance of the crystal greater than 10. This assure that we really are in the conditions of undepleted pump approximation in which the theoretical model was established. Due to the large sensitivity of the CCD camera this condition was easy to satisfy.

II.2. The photorefractive crystal

The photorefractive crystal is an antireflection-coated iron doped BaTiO_3 crystal in a classical geometry, i.e. with the C-axis perpendicular to the entrance face. The external angle between the beams is of the order of 20° and the crystal is tilted in order to take advantage of the high r_{42} electrooptic coefficient (the tilt is such that the pump beam is incident quasi normally on the crystal). For each experiments the crystal is fully characterized with respect to the photorefractive parameters. A typical set of the experimental parameters is presented in Table 1. They are the ones used in the theoretical calculations which also corresponds to the experiments presented here.

The photorefractive gain is evaluated through a measurement of the attenuation of the signal beam. For the determination of the response time of the photorefractive crystal, we write a grating that gives an attenuation of the signal beam. Then the signal beam is turned off for a short period of time and the response is recorded on a Silicon detector positioned in place of the CCD camera (Fig. 3). This signal corresponds to the response of the beam coupling set-up to an intensity novelty. We thus use the theoretical model (eq. (12)) to adjust the experimental results. The only unknown parameter being the response time we use this adjustment to determine this response time. We measure $\tau_0=750\text{ms}$, with an excellent accordance between the experimental and the theoretical curves (Fig. 4).

The photorefractive gain - interaction length product ($\gamma \times l = 2.83$) of our crystal is clearly not sufficient to obtain an optimized implementation of the photorefractive novelty filter. Much higher gain could have been obtained with higher tilting angle of the crystal, but

we have another constraint on the choice of the angle, which is the obligation to transmit the whole image of the SLM without diaphragmation and to cover this image with the pump beam. This imposes moderate incidence and tilting angles and thus a moderate photorefractive gain, nevertheless the gain is sufficient for a good operation of the novelty filter. As we will show, the operation is in fact not limited by this rather moderate gain but by the flicker of the SLM that reduces the apparent attenuation of the signal beam and thus the performances of the novelty filter.

II.3. The spatial light modulator

The SLM is issued from an Epson video projector. It is used as a phase modulator and was characterized in this regime. The method and results of this characterization of the SLM are presented elsewhere [11] but the important point is that quasi pure linear phase modulation has been obtained with a very small known residual intensity modulation. Two regimes of operation of the SLM are used (Fig. 5). One where a linear phase modulation between 0 and 1.3π is obtained, it will be called in the following the “0” contrast regime (by reference to the adjustment of the SLM electronics). The second regime gives a quasi linear phase modulation between 0 and 2.5π , this will be the “10” contrast regime. Curves in Fig. 5 give a perfect knowledge of the value of the amplitude (in phase and intensity) of the signal beam for any value of the grey level. These values will be used for the calculation of the theoretical curves.

This SLM presents a flicker due to the leakage of the transistors that are supposed to apply the voltage to the liquid crystal cells. The phase modulation is thus modulated at a frequency corresponding to the refreshing period of the transistors (i.e. 25Hz in our case). This phase variation is seen by the novelty filter as a permanent novelty always present on the signal and it will be of course detected as a novelty. Practically it is responsible for a reduction of the apparent attenuation of the signal beam and thus for reduced performances of the novelty filter (due to the presence of a high amplitude noise). This is clearly visible in Fig. 6, where we see the attenuation of the signal beam with the SLM off, and with the SLM on with different uniform grey level applied on it.

First the flicker is at twice the period of the refreshing of the SLM (due to the quadratic response of the photorefractive crystal in the diffusion regime to a periodic phase modulation [5-7]). Second there is a reduction of the apparent attenuation of the signal beam (given by the average value of the detected signal). This reduction is all the more important as the grey level is important as the flicker noise increases with the grey level. It should be noted that the model we developed enables to take this flicker noise into account (as will be seen in the following). It can even be used to deduce the value of the photorefractive gain from the data of Fig. 6. From the “noisy” curves of Fig. 6 we measure $\gamma=(7.8\pm 0.2) \text{ cm}^{-1}$, and estimate

the amplitude of the flicker noise phase modulation (0.5rad for the 255 level and 0.25rad for the 100 level, both case corresponds to the worst case of a “10” contrast regime).

Looking now at the attenuation of the image we goes from a 175 times attenuation without the SLM to a 8 times attenuation with the SLM on (255 level uniform image with a “10” contrast). This is clearly seen on the images in Fig. 7. For this experiment we insert a slide with a chessboard image just in front of the SLM to simulate the image and put an uniform image on the SLM (255 grey level with “10” contrast). The initial image is seen in Fig. 7.A and the attenuated image in Fig. 7.B, without changing anything to the set-up. The attenuation seems good but an enhancement of the contrast of the attenuated image, with a simple image processing computer program clearly reveals the image (Fig. 7.C). The same experiment, performed with the SLM off (SLM driver turned off), shows that in order to begin to guess the image after contrast enhancement (Fig. 7.E), the initial image (without attenuation) has to be greatly saturated (Fig. 7.D). The loss of the apparent attenuation due to the flicker is thus clearly seen in these images. These images also show the good quality of our imaging optics. The residual distortion is mostly due to dust on the optics, that have not been totally eliminated and that gives fringes structures, and to defects inside the photorefractive crystal, giving scattering points on the attenuated image.

We perform some measurements of the temporal response of the SLM using the residual amplitude modulation observed in the phase modulation regime. We measure an exponential response of the SLM, with a time constant roughly estimated around 80ms. We just make a rough estimation of the time constant because a precise determination of this response time is very difficult due to the flicker of the SLM, which varies on time scale close to the response time of the SLM. The estimated response time corresponds to what was previously observed, i.e. a build-up of the phase shift until its maximum in about 2 images [12].

II.4. Discussion

The set-up used as a two beam coupling photorefractive novelty filter has been presented and characterized. All the parameters of the set-up, essentially the photorefractive crystal parameters, are known as well as the image parameters, essentially the response of the SLM. The defects of the SLM might even be taken into account as we know that the SLM presents flicker and it can be introduced into the modelization, together with the response time constant of the SLM (even if the found value has a great uncertainty). All these parameters will be introduced in the theoretical model to calculate the response of the novelty filter. The comparison with the experimental response will be thus performed without having any free parameters (they are all determined more or less precisely by independent experiment).

III. EXPERIMENTAL RESULTS

To determine the performances of the photorefractive novelty filter, we send to the SLM computer generated series of images using a frame grabber connected to the SLM. The sequence of images is the following : first an uniform image with a level n_0 followed at time $t=0$ by a second image constituted of a 50pixels x 50pixels square with level $n_1 = n_0 + \Delta n$. Then after about 1s once again the initial background image is sent. In the experimental set-up the CCD camera is replaced by Si detector which surface is fully covered by the image of the square. The experimental study concentrates on the response of the novelty filter to the amplitude of the novelty Δn and on the influence of initial level n_0 .

III.1. Response to the amplitude of the novelty

We here fix the initial level $n_0 = 0$ and vary Δn . In the first experiment the contrast of the SLM is set to “0”, which means that we have a linear response of the SLM with a maximum amplitude of the phase variation of about 1.3π . The experimental results are presented in Fig. 8 (all the curves here and in the following are single shot curves). The temporal structure of the curves corresponds to the theory. At the appearance of the square (at $t=0$) the novelty filter detects it and, then it adapts to the new image, what corresponds to the disappearance of the novelty peak. Then the square disappears which gives a new peak as this disappearance is also a novelty. Then this peak disappears as the novelty filter readapts to the new image. The amplitude of the novelty peaks varies as the square root of the novelty amplitude (Fig. 8.F) as predicted by the theory (in the case considered here of linear dependence of the phase shift with grey level). The saturation (and the departure from the straight line) at high grey level change is due to the high value of the phase change, with such high value (around $\pi/2$) the influence of the sinus function (given by relation (33)) begins to appear. Moreover, we see in Fig. 8 the good accordance of the experimental curves with the calculated ones (reminding that the theoretical curves are calculated one and that no adjustment is performed).

The same measurement is performed with the SLM contrast at level “10” (Fig. 9) where the maximum phase variation is greater than 2π . Here again we have a good accordance between the experimental curves and the calculated ones. We see the peculiar behaviour predicted by the theory (Fig. 2). For example, for the curve with $n_1 = 150$, corresponding to a phase variation of 2π , we observe the transient response due to the finite response time of the SLM. The accordance between calculated curves is good even if a more precise adjustment could have been made, just playing with the value of τ_R (as already seen in Fig. 2), and confirmed by curve at $n_1=200$ calculated with a smaller value of τ_R (30ms instead of the roughly estimated value of 80ms (§II.4.)) and showing a better accordance with

experiment. Nevertheless, whatever the exact value of this response time the feature of the curve is always the same. One can also note that the height of the transient peaks at high modulation overpasses the initial intensity of the signal beam (obtained without pump beam) as predicted by the theory (even if it is reduced compared to the 4 fold amplification predicted by the theory due to the finite response time of the SLM). These curves also show that it is possible to detect a novelty amplitude as low as 10 grey levels, despite the high level of fluctuations (due in fact to the flicker of the SLM as will be seen later).

III.2. Independence of the response towards the initial level

A peculiarity of the use of a phase modulation to introduce the image into the novelty filter, is the independence of the response towards the initial level. Thus we conduct measurements where we keep a constant novelty amplitude (of opposite sign compared to previous measurements) and vary the initial level n_0 . The contrast is set at “0” to have a linear response of the SLM. The curves (Fig. 10) show that the amplitude of the novelty peaks stays constant whatever the initial level (the smaller signal at low initial level ($n_0=50$) being certainly due to the small sublinearity of the response of the SLM at small grey levels (Fig. 5)).

To confirm this advantage of phase modulation against intensity modulation operation of the novelty filter, we perform the same experiment with an intensity modulated beam. The experimental conditions were slightly different as we use plane waves and an acousto-optic modulator to perform the experiment (and the parameters of the crystal (γ and τ_0) were slightly different). The ratio of the amplitude of the novelty compared to the maximum accessible amplitude is similar to the one in the previous measurements for a good comparison between both experiments. We change the initial level from a low level, towards a medium and a high level. We see (Fig. 11) that the amplitude of the peaks is greatly reduced when the initial level increases, indicating that, as predicted by the theory, it is easier to detect a novelty on a black level than on a white level. Again, the accordance between experimental curves and theoretical ones is good.

III.3. Comparison with theory

As seen previously for all the experimental curves we can simulate exactly the response of the novelty filter, and compare it to the experimental results. As we have seen the accordance is rather good whatever the experimental conditions, especially in the case of an intensity modulated signal beam (Fig. 4 and Fig.11), what validates our theoretical model. However our model allows to go even farther. Indeed we notice that the curves in the phase modulation regime are characterized (especially at low novelty amplitude) by a strong “noise”

that limits the performances. Thanks to the model we can now explain this “noise” that is not a real noise but is rather due to the fluctuations of the SLM.

This flicker of the SLM is known, it can be modeled as a sinusoidal phase modulation with period 40ms (Fig. 6) and with an amplitude that varies with the grey level. We will take it equal to 0.2rad for our simulation. We add this additional phase modulation to the initial variation of the incident signal beam $E_d(0,t)$ in our simulations in order to calculate the real response of the SLM and to compare it to the experiment. For this comparison (Fig. 12) we take as experimental data the curve in Fig. 8.C. The accordance between calculated and measured curves is very good, the exact feature of the response of the novelty filter being modeled. We can also see that the previous calculated curve (that does not take into account the flicker) gives nevertheless a good idea of the averaged amplitude of the novelty signal, confirming the quality of the previous simulations.

III.4. Discussion

Our results are important because they confirm the validity of our theoretical model of the photorefractive two beam coupling novelty filter. It is now possible to modelize the behaviour of the novelty filter when changing the performances of the different components of the set-up and to optimize the response. Moreover new features have been discovered that allow to operate with phase shifts greater than 2π , by using the finite response time of the SLM. This new working regime will have to be explored in more details in order to implement future versions of the system.

The results are also important because they show that the “noise” that limits the performances of the novelty filter for the detection of small grey level variation, is in fact due to the SLM. This means that the use of better SLM that does not exhibit such a flicker, would increase the performances of the system. Such spatial light modulators commercially exist [13] and will be chosen for future implementation of such novelty filters.

IV. CONCLUSION

We have performed both theoretical and experimental evaluations of the performances of a photorefractive two beam coupling novelty filter. The theoretical model allows to deduce that the operation of this kind of filter is greatly improved if the image is imprinted on the signal beam as a phase modulation rather than as an intensity modulation. In such a case, the requirements on the photorefractive crystal (essentially the photorefractive gain) are greatly reduced, but also the response of the novelty filter to small changes in the image becomes totally independent of the initial level of the pixel. In other words, it is as easy to detect a one grey level variation on a “white” background as on a “black” background. This is of importance as the main application of this kind of system is the detection of small objects

appearing or moving in a highly textured scene. These theoretical predictions are confirmed by the experiments we performed, all the predicted features being perfectly observed experimentally.

Apart this result, the model gives perfect simulations of the operation of the novelty filter. The calculated curves are indeed in excellent accordance with the experimental ones. This agreement allows to show that the main limitation of our set-up was in fact due to the spatial light modulator we used, and particularly its flicker. This limitation is important and an operating system will have to be built with new generation SLMs that do not present this flicker. Taking into account the model we developed, we are now able to simulate the response of the system when changing one element or the other and to predict the performances of the novelty filter with these new elements.

Acknowledgments :

Support for this research by Direction des Systèmes de Forces et de la Prospective of DGA is greatly acknowledged.

References

- [1] M. Cronin-Golomb, A.M. Biernacki, C. Lin, H. Kong, "*Photorefractive time differentiation of coherent optical images*". Opt. Lett. **12**, 1029 (1987).
- [2] D.Z. Anderson, J. Feinberg, "*Optical novelty filters*". IEEE. J. Quantum Elec. **25**, 635 (1989).
- [3] M. Sedlatschek, T. Rauch, C. Denz, T. Tschudi. "*Demonstrator concepts and performances of a photorefractive optical novelty filter*". Opt. Mat. **4**, 376 (1995).
- [4] P. Mathey, P. Jullien, A. Dazzi, B. Mazué. "*Performance evaluation of a photorefractive novelty filter for motion tracking and edge enhancement*". Opt. Commun. **129**, 301 (1996).
- [5] Ph. Delaye, L.A. de Montmorillon, G. Roosen. "*Transmission of time modulated optical signals through an absorbing photorefractive crystal*". Opt. Commun. **118**, 154 (1995).
- [6] Ph. Delaye, A. Blouin, D. Drolet, L.A. de Montmorillon, G. Roosen, J.P. Monchalin. "*Detection of ultrasonic motion of a scattering surface using photorefractive InP:Fe under applied DC field*". J. Opt. Soc. Am. B **14**, 1723 (1997).
- [7] L.A. de Montmorillon, Ph. Delaye, J.C. Launay, G. Roosen. "*Novel theoretical aspects on photorefractive ultrasonic detection and implementation of a sensor with an optimum sensitivity*". J. Appl. Phys. **82**, 5913 (1997).
- [8] M. Abramowitz, I.A. Stegun, "*Handbook of mathematical functions*". Eds. Dover (New York)
- [9] A. Hermanns, C. Benkert, D.M. Lininger, D.Z. Anderson, "*The transfer function and impulse response of photorefractive two-beam coupling*". IEEE. J. Quantum Elec. **28**, 750 (1992).
- [10] L. Mager, C. Laquarroy, G. Pauliat, M.H. Garrett, D. Rytz, G. Roosen. "*High quality selfpumped phase conjugation of nanosecond pulses at 532nm using photorefractive BaTiO₃*". Opt. Lett. **19**, 1508 (1994).
- [11] Ph. Delaye, G. Roosen. "*Simple technique for the determination of the complex transmittance of spatial light modulator*". To be published in Optik (1998).
- [12] C. Soutar, S.E. Monroe, J. Knopp, "*Measurement of the complex transmittance of the Epson liquid crystal television*". Opt. Eng. **33**, (1994) 1061.

- [13] D.J. Cho, S.T. Thurman, J.T. Donner, G.M. Morris. “*Characteristics of a 128x128 liquid crystal spatial light modulator for wavefront generation*”. Opt. Lett. **23**, 969 (1998).

Figure Captions

Figure 1 : Schematic of two beam coupling in a photorefractive crystal.

Figure 2 : Response to a phase change that establishes with an exponential law of increasing response time ($\tau_R=3\text{ms}$ plain line, $\tau_R=30\text{ms}$ dotted line, $\tau_R=80\text{ms}$ dashed line). The steady state phase shift change is 0.5π (curves A), 2π (curves B) and 2.5π (curves C). The transmitted signal when the novelty filter does not work is 100. The crystal parameters for the calculation are $x=3.63\text{mm}$, $\alpha=0.7\text{cm}^{-1}$, $\gamma=-7.8\text{cm}^{-1}$ and $\tau_0=750\text{ms}$.

Figure 3 : Experimental set-up of the photorefractive two beam coupling novelty filter. $\lambda/2$ is an half wave plate, P a dichroic polarizer, PBS a polarizing beam splitter, OI an optical isolator, and SLM is the spatial light modulator.

Figure 4 : Signal given by the novelty filter, when the signal beam is turned off during 181ms. The signal beam power in the absence of the pump beam is 96mV. The dotted line represents the theoretical curve. The offset between the curves is for clarity of presentation. For this experiment the SLM was turned off and has no action on the beam.

Figure 5 : Experimental values of the phase shift (black markers) and transmission in amplitude (grey markers) of the SLM as a function of the grey level, for “0” contrast (+) and “10” contrast (Σ).

Figure 6 : Experimental curve of the attenuation of the signal beam with the SLM off (A) and the SLM on (B). On (A) the insert shows temporal response of the attenuated signal. (B) shows the temporal response of the attenuated signal for different levels n of the uniform image sent on the SLM (contrast “10”).

Figure 7 : Attenuation of an image imprinted on the signal beam with the SLM on (uniform image with level $n=255$, with contrast “10”) (A, B, C) and with the SLM off (D, E). Images A and D are taken before attenuation, and images B, C and E are taken after attenuation and after an identical contrast enhancement for images C and E.

Figure 8 : Experimental curves (grey curves) of response of the novelty filter to an increasing novelty amplitude between a level $n_0=0$ and a level $n_1 = n_0 + \Delta n$ (A :

$n_1=50$, B : $n_1=100$, C : $n_1=150$, D : $n_1=200$, E : $n_1=250$), the contrast of the SLM is “0”. The black curves are calculated theoretical curves. Figure F shows the variation of the square root of the height of the first peaks versus the grey level variation Δn .

Figure 9 : Experimental curves (grey curves) of response of the novelty filter to an increasing novelty amplitude between a level $n_0=0$ and a level $n_1 = n_0+\Delta n$, the contrast of the SLM is “10”. The black curves are calculated theoretical curves using a response time of the SLM $\tau_R=80\text{ms}$. The dashed line for $n_1=200$ corresponds to a calculated theoretical curves using a response time of the SLM $\tau_R=30\text{ms}$. The signal power without the pump beam is 86mV.

Figure 10 : Experimental curves of response of the novelty filter to a constant novelty amplitude ($\Delta n=50$) between a varying level n_0 and a level $n_1 = n_0-\Delta n$. The contrast of the SLM is “0”.

Figure 11 : Experimental curves (grey curves) of response of the novelty filter to a quasi constant intensity variation on different initial levels. The incident signal is shown on the curves and has been horizontally shifted for clarity. The black curves are calculated theoretical curves. The intensity modulation is obtained with an acoustooptic modulator that replaced the liquid crystal SLM.

Figure 12 : Comparison between the experimental curve of Fig. 8.C and the theoretical curve (dotted line), taking into account the exponential response time of the SLM $\tau_R=80\text{ms}$ and the additional phase modulation due to flicker. The theoretical curves presented in Fig. 8.C is also given (dashed line), it takes into account the exponential response time of the SLM but not the flicker. Without the pump beam the signal power is 86mV. The offset between the curves is for clarity of presentation.

Table

x (mm)	3.63
α (cm ⁻¹)	0.7
γ (cm ⁻¹)	-7.8
τ_0 (ms)	750

Table 1 : Typical set of the parameters of the photorefractive crystal used in the experiment.

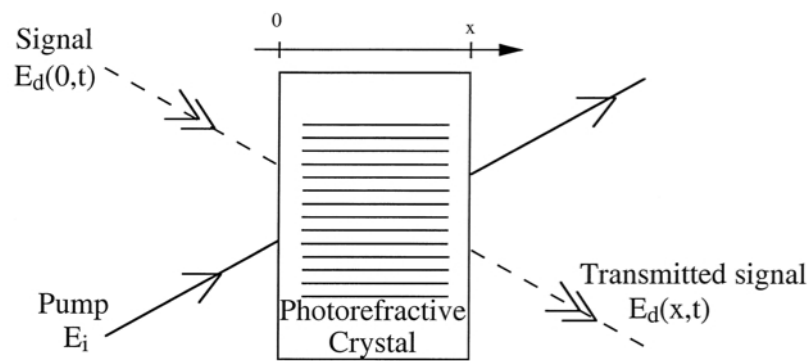


Figure 1

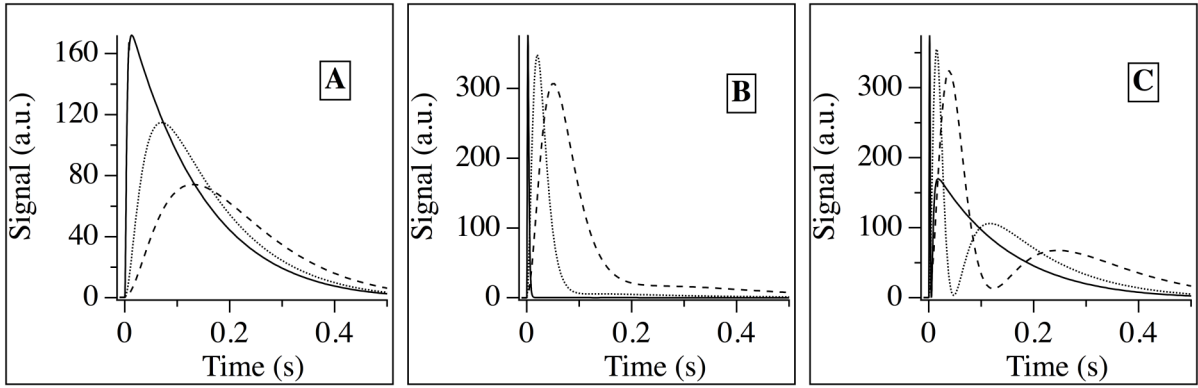


Figure 2 : Delaye et al.

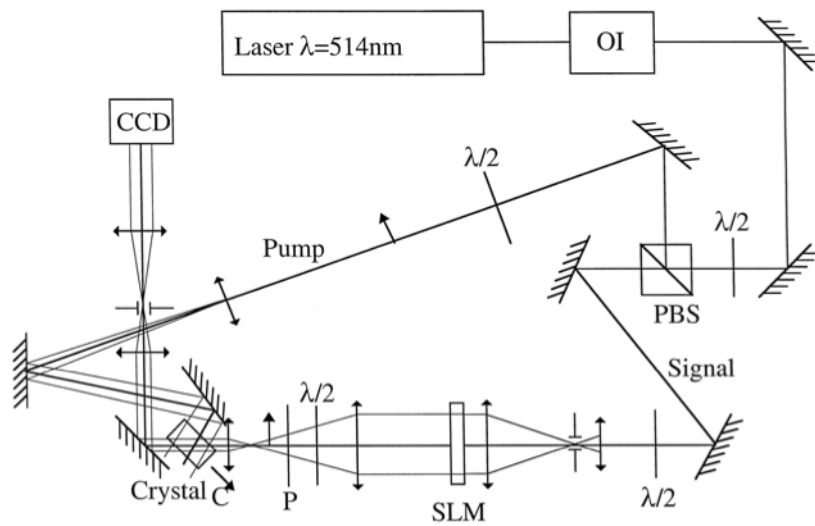


Figure 3

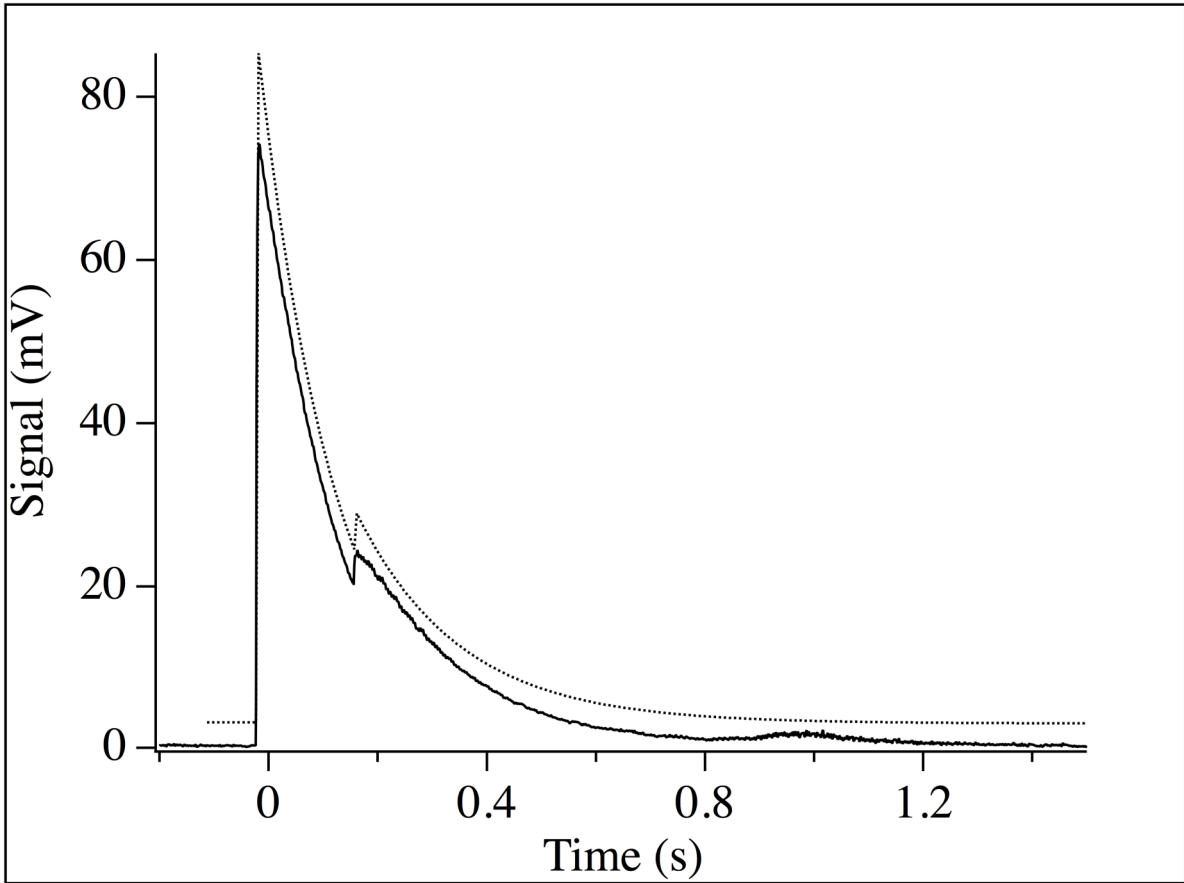


Figure 4 : Delaye et al.

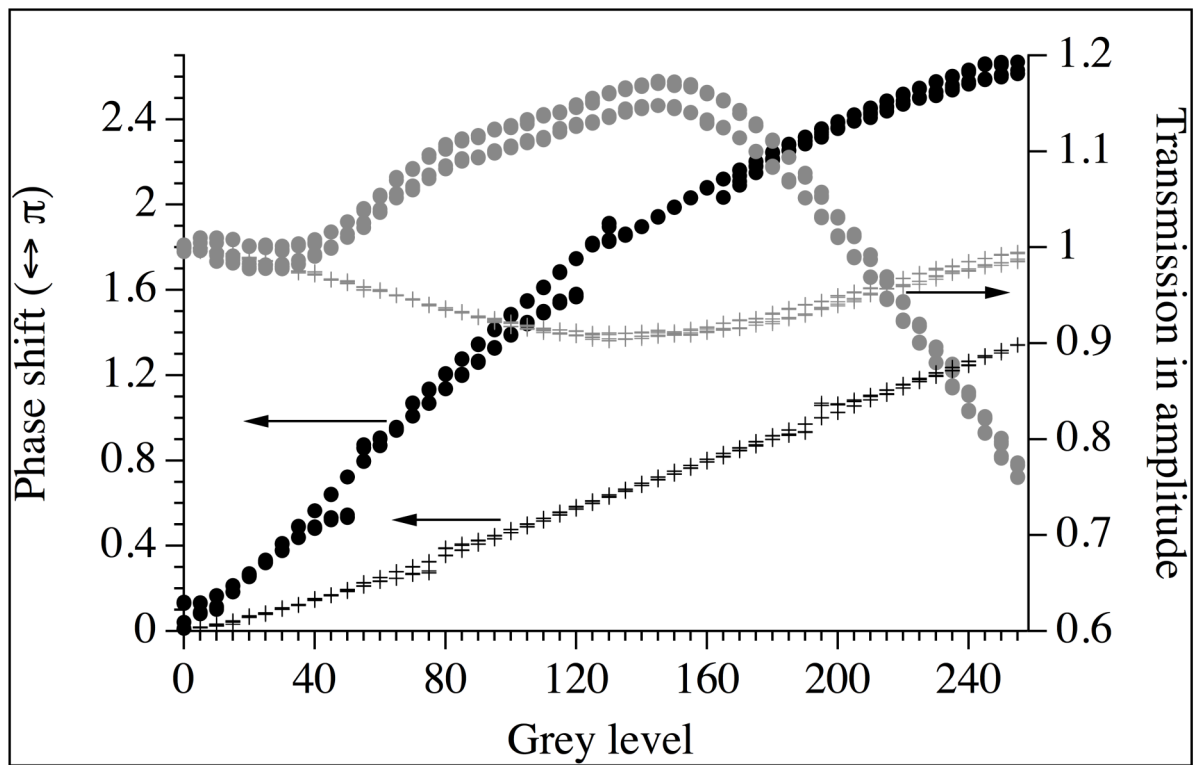


Figure 5 : Delaye et al.

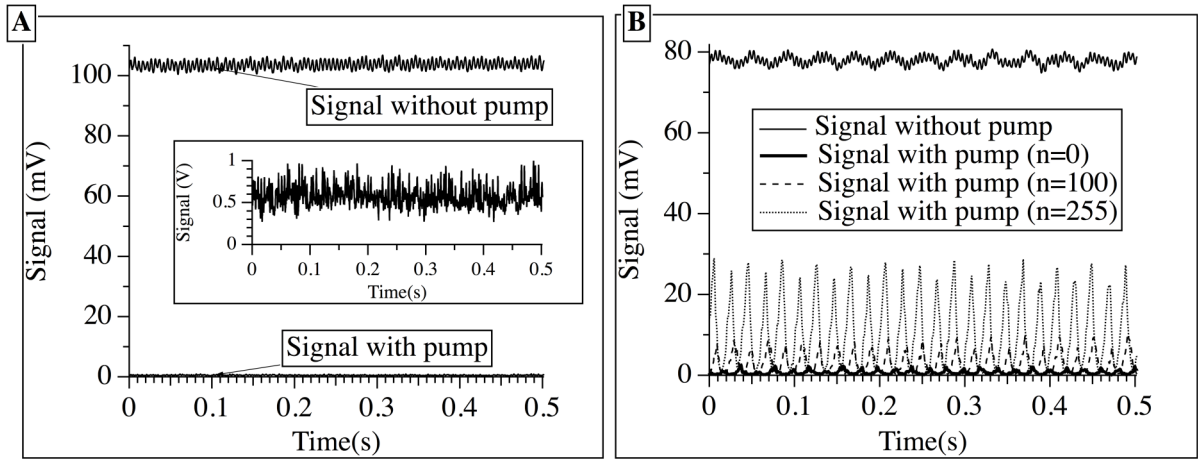


Figure 6 : Delaye et al.

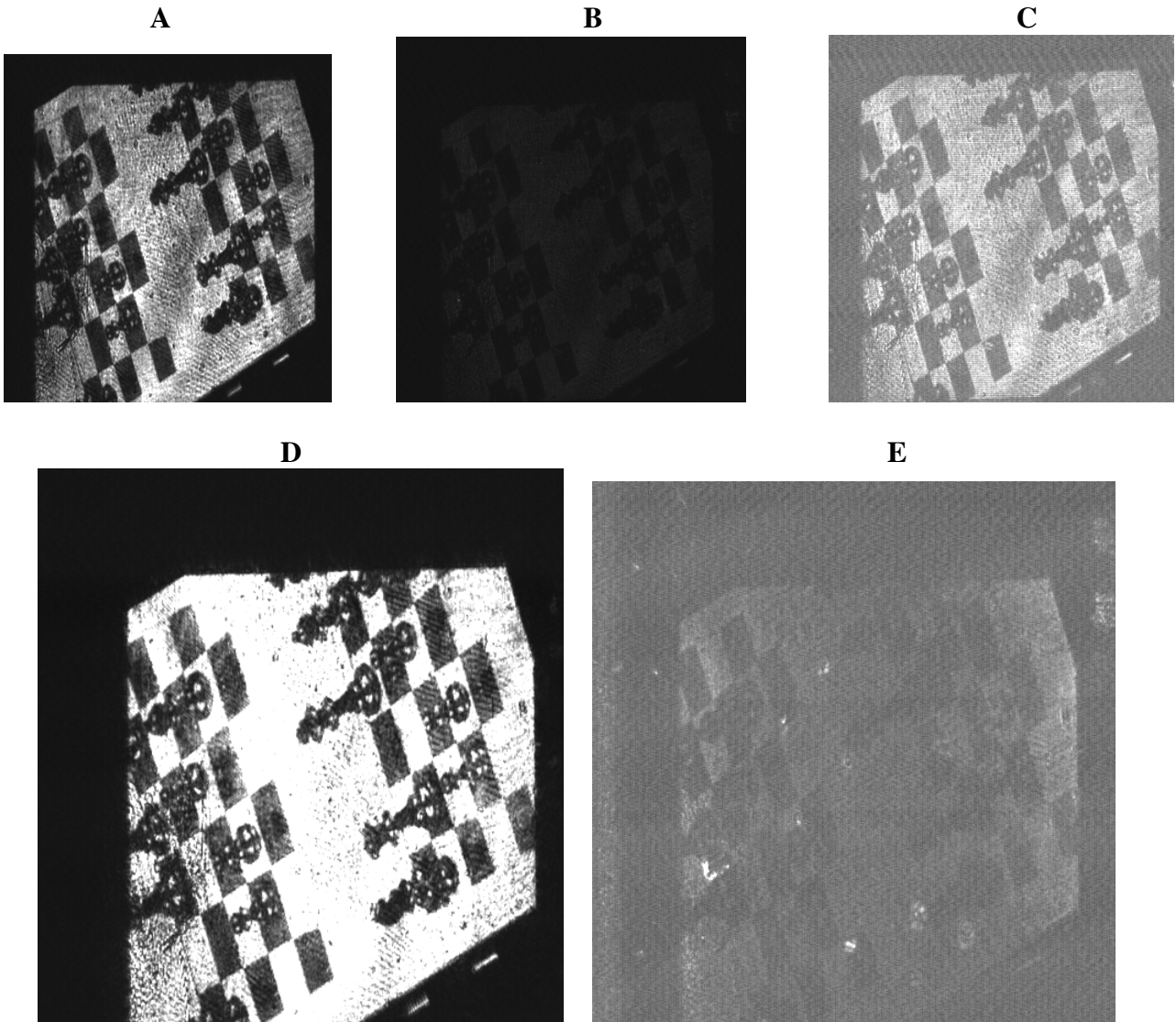


Figure 7 : Delaye et al.

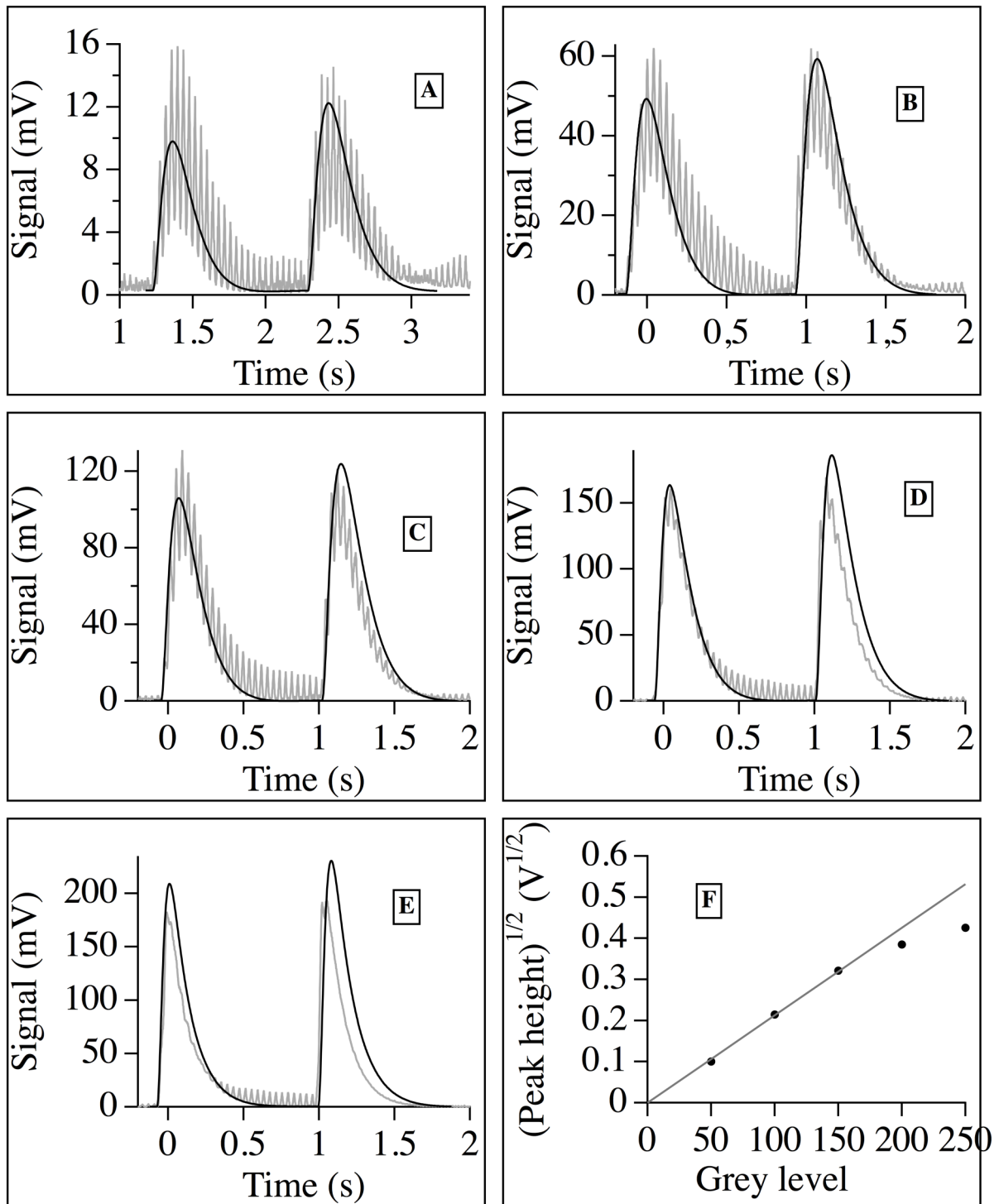


Figure 8 : Delaye et al.

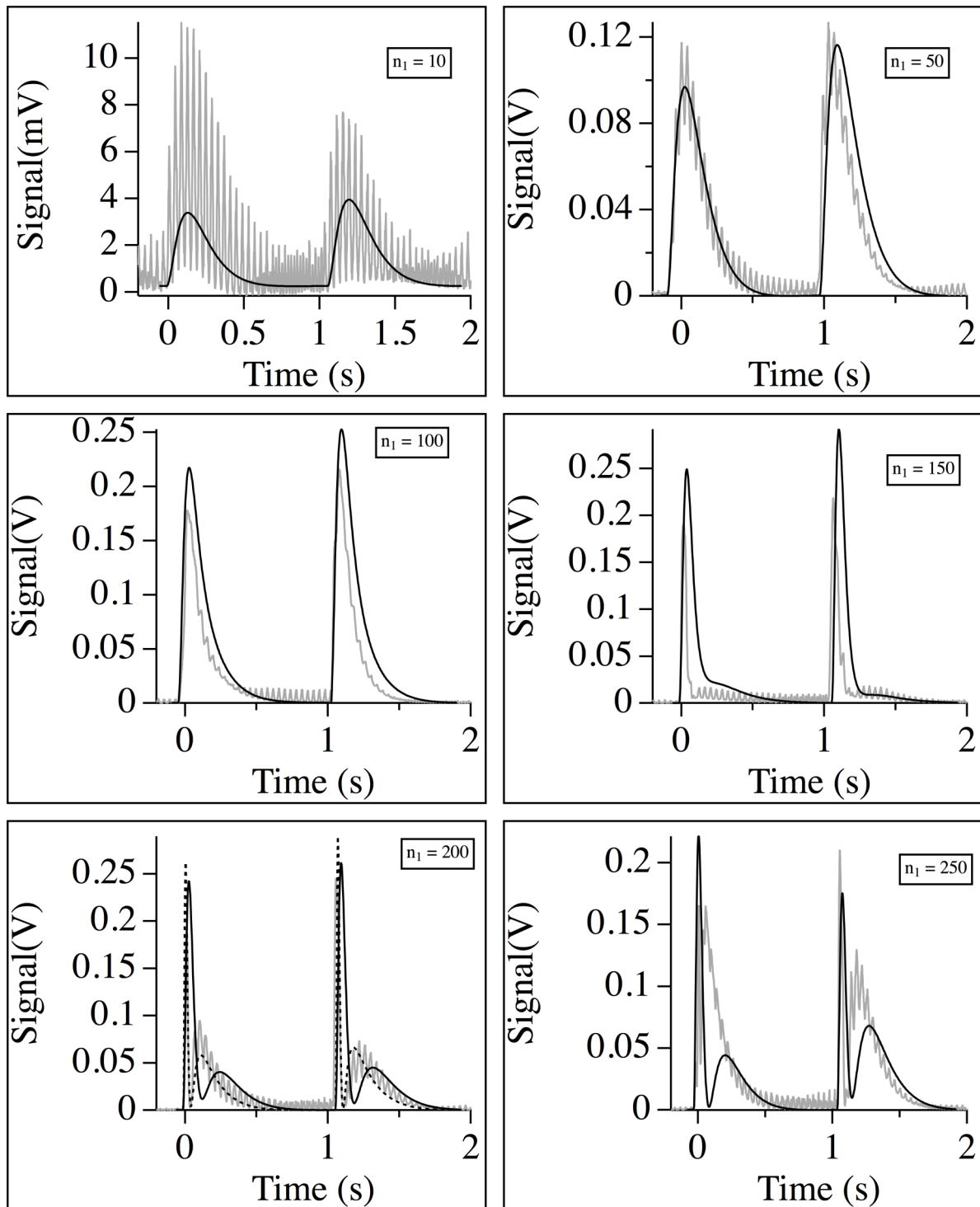


Figure 9 : Delaye et al.

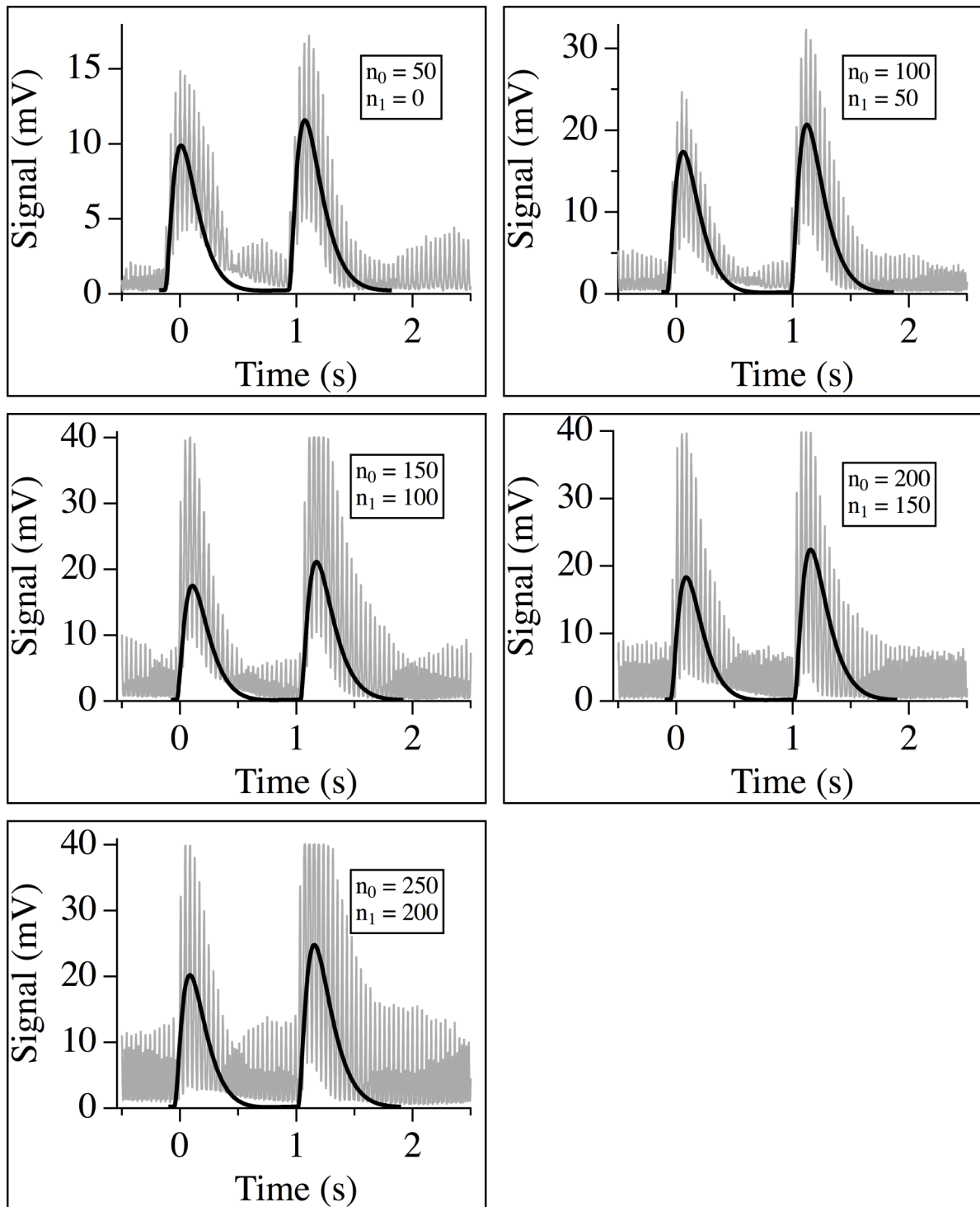


Figure 10 : Delaye et al.

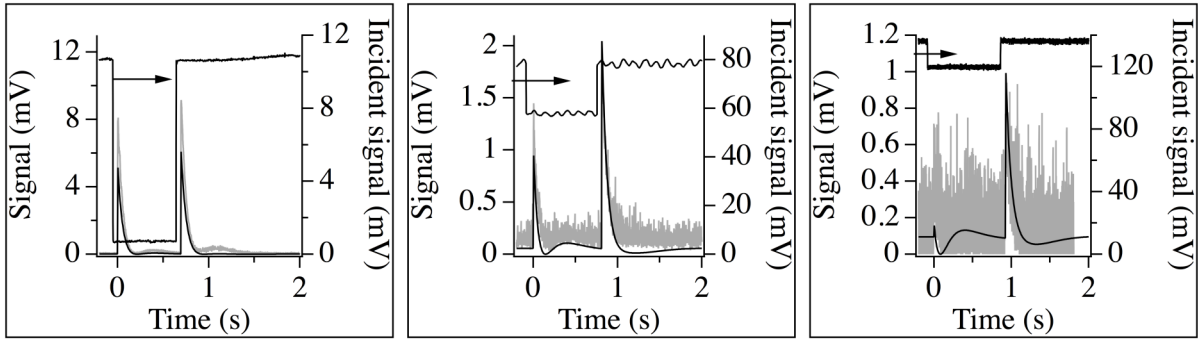


Figure 11 : Delaye et al.

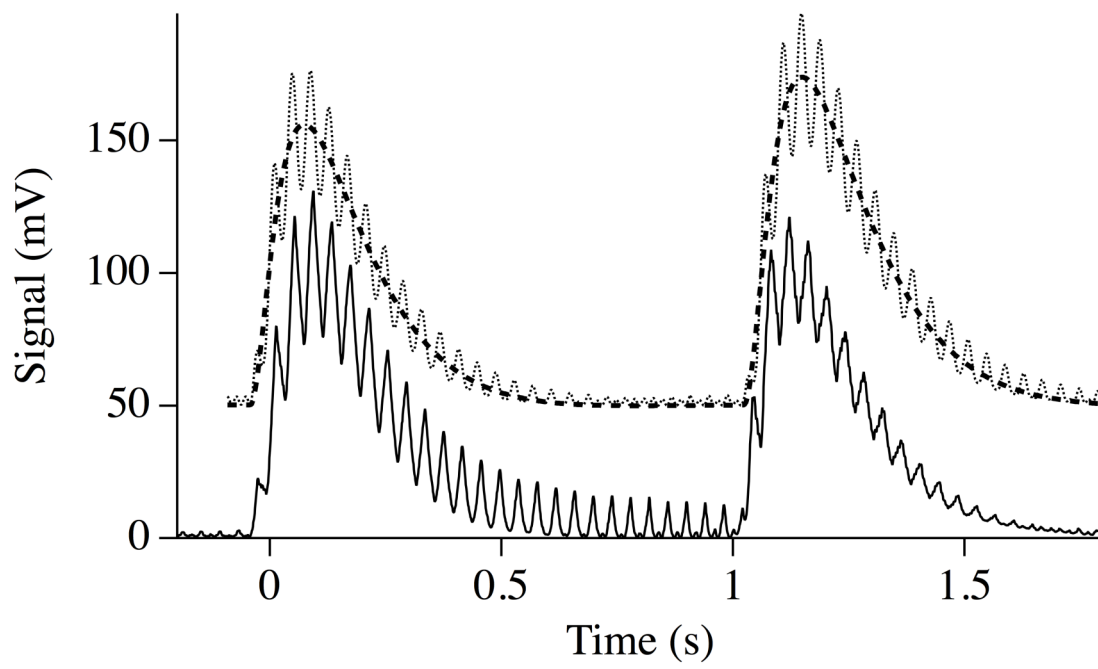


Figure 12 : Delaye et al.